The H_2O line shifts induced by nitrogen, oxygen and air pressure within the impact theory by Anderson

A.D. Bykov, N.N. Lavrentieva, and L.N. Sinitsa

Institute of Atmospheric Optics,
Siberian Branch of the Russian Academy of Sciences, Tomsk

Received July 20, 1999

The water vapor line shift coefficients were calculated and the analysis of main factors, affecting the value and sign of a shift was performed, using the Anderson impact theory. The vibrational and rotational dependences and the role of different terms of intramolecular potential was analyzed. It was shown that the compensation for different scattering channel contributions defines the variation of the shift coefficients with the increasing quantum number. In the calculations one fitted parameter, the mean dipole polarizability of the upper vibrational state, has been used. Calculations are in a satisfactory agreement with the experimental data.

I. Introduction

There is a growing interest in measurements of line shifts of the atmospheric gases and in calculations including water vapor. Accurate H_2O line shifts induced by N_2, O_2, and air pressure are necessary for atmospheric optics applications. Investigation of H_2O absorption line broadening and shifts is of current interest for the problems of remote sounding of atmospheric humidity fields by the differential absorption method.[1] Neglecting the H_2O line shift by air pressure can lead to systematic errors of 30 to 100% in retrieving the water vapor concentration at altitudes from 15 to 20 km.[2]

At present the shift coefficients induced by pressure of different foreign gases were measured for many lines from MW to the visible spectral range.[3–15] The experimental results available allow one to conclude that line shift has more complicated features when compared with line broadening and many non-essential for the width factors become important for the shift. It is confirmed, for instance, by the fact of strong dependences of line shift coefficient on vibrational quantum number, type of foreign gas molecules, isotopic specie as well as temperature and pressure of the sample.[3,14,16] As was noticed in Ref. 14, the line pressure shift coefficients can become the promising tool in molecular collision studies, since the pressure shift is more sensitive to the intramolecular interaction parameters and details of intramolecular motion than the line broadening.

Theoretical investigations of the water vapor line shifts are presented by several calculations within the framework of Anderson method,[17,18] QFT-method,[19] and Full Complex Robert–Bonamy (FCRB) theory,[20–24] but many published experimental results were not explained up to now. It is worth noting here that the accurate FCRB calculations were performed only for ν_2, ν_1, ν_3, $3\nu_1 + \nu_3$, and $2\nu_1 + 2\nu_2 + \nu_3$ bands, the Anderson calculations were performed for MW,[18] ν_2, and some bands in the near IR and visible regions.

This paper is aimed at the analysis of different factors, which play an important role in the H_2O line shifts calculations. The calculations were performed by two methods: the Anderson one[25,26] and cut-of-free[27] theory, not using perturbation theory in scattering matrix elements calculation. Henceforth, for the sake of brevity, we shall name it as Cherkasov method. Since the results of calculations were found to be close in general, we have used the Anderson theory to make the result of analysis more illustrative.

The analysis is organized as follows. In section II the brief outline of theoretical background and details of calculations is presented. Section III contains applications to the H_2O molecule. The first and second parts are devoted to the analysis of vibrational and rotational dependences of the line shift coefficients. Analysis of the last part is based on the consideration of scattering channel contributions. In the end of the third section large array of measured and calculated data for different H_2O bands and different perturbing particles is presented.

II. Theoretical background and details of calculations

The semiclassical impact theories by Anderson[25,26] and Cherkasov[27] were used for the water vapor line shifts calculations. As usual, the general assumptions are the following: collisions are considered as binary, the duration of a collision is less than the time between collisions, the translational motions of particles are treated following the classical paths approximation, no line mixing effects occur. In this case the spectral line halfwidth γ_{if} and the line center shift δ_{if} for the transition $i \to f$, where i and f are the sets of quantum numbers of the initial and the final states, are given by the following formula[26]:

$$\gamma_{if} + i\delta_{if} = \frac{n}{c} \sum_2 \rho(2) \int_0^\infty dv\, v\, f(v) \int_0^\infty db\, b\, S(b), \quad (1)$$

0235-6880/99/10 919-09 $02.00

where $i \equiv \alpha_i j_i m_i$; $f \equiv \alpha_f j_f m_f$; 2 ($2 \equiv \beta l \mu$) denotes the set of quantum numbers of perturbing molecule (j are quantum numbers of angular momentum, m are magnetic quantum numbers, and α are all other quantum numbers), n is the density of a buffer gas, $f(v)$ is the Maxwell distribution function, b is the impact parameter. According to Ref. 28, the general expression for efficiency function $S(b)$ is as follows:

$$\begin{aligned} \mathrm{Re}\, S(b) &= 1 - [1 - \mathrm{Re}\, S_2'^{\,\mathrm{middle}}(b)] \exp\{-\mathrm{Re}\, S_2^{\mathrm{outer}}(b) + \\ &+ S_2''^{\,\mathrm{middle}}(b)\} \cos\{\mathrm{Im}\, S_2^{\mathrm{outer}}(b) + S_1(b)\}; \\ \mathrm{Im}\, S(b) &= [1 - \mathrm{Re}\, S_2'^{\,\mathrm{middle}}(b)] \exp\{-\mathrm{Re}\, S_2^{\mathrm{outer}}(b) + \\ &+ S_2''^{\,\mathrm{middle}}(b)\} \sin\{\mathrm{Im}\, S_2^{\mathrm{outer}}(b) + S_1(b)\}, \end{aligned} \quad (2)$$

where $S_1(b)$, $S_2(b)$ are the well known first- and second-order "interruptionB functions from the Anderson theory. Primed and doubly primed terms correspond to BlinkedB and BconnectedB diagram contributions of the perturbation theory.

The interruption function in the Anderson method results from perturbation expansion and can be represented as

$$S(b) = S_1(b) + S_2(b) + \dots . \quad (3)$$

The first-order term $S_1(b)$ is responsible for the adiabatic effect and is defined by the isotropic part of the intermolecular potential only. In the case of collision polar H_2O molecule with non-polar molecule N_2, the $S_1(b)$ term can be written as

$$S_1(b) = -\frac{3\pi}{8\hbar v b^5}\,\alpha_2 \left\{ \langle V_i | \mu^2 | V_i \rangle - \langle V_f | \mu^2 | V_f \rangle + \right.$$
$$\left. + \frac{3\varepsilon\varepsilon_2}{2(\varepsilon + \varepsilon_2)} [\langle V_i | \alpha | V_i \rangle - \langle V_f | \alpha | V_f \rangle] \right\}. \quad (4)$$

In Eq. (4) α, μ, and ε are the polarizability, dipole moment, and ionization potential of the H_2O molecule, respectively, α_2 and ε_2 are the polarizability and ionization potential of the perturbing molecule. The second-order term consists of three parts:

$$S_2(b) = S_{2i}^{\mathrm{outer}}(b) + S_{2f}^{\mathrm{outer}}(b)^* + S_2^{\mathrm{middle}}(b), \quad (5)$$

where

$$S_{2i}^{\mathrm{outer}}(b) = \sum_{l_1 l_2} \frac{A_{l_1 l_2}}{\hbar^2 v^2 b^{2(l_1 + l_2)}} \sum_{2'} D^2(22' | l_2) \times$$
$$\times \sum_{i'} D^2(ii' | l_1)\, \varphi_{l_1 l_2}(k_{ii'22'}); \quad (6)$$

the term $S_{2i}^{\mathrm{outer}}(b)$ is obtained from Eq. (6) replacing i by f; l_1 and l_2 denote the type of interaction: $l_1 = 1$, $l_2 = 1$ correspond to dipole-dipole interaction, $l_1 = 1$, $l_2 = 2$ correspond to dipole-quadrupole interaction, an asterisk means the complex conjugate value;

$$D^2(ii' | l) = (\nu_i j_i r \| T_l \| \nu_i' j_i' r')^2 / (2j_i + 1) \quad (7)$$

are the transition moments and $(\nu_i j_i r \| T_l \| \nu_i' j_i' r')$ are the reduced matrix elements of the irreducible tensor operator T_l of the rank l; r and r' denote the sets of all other quantum numbers except for J. The factors $A_{l_1 l_2}$ are chosen in such a way that $\mathrm{Re}\, \varphi_{l_1 l_2}(0) = 1$; $\varphi_{l_1 l_2}(k_{ii'22'})$ are the complex resonance functions

$$\varphi_{l_1 l_2}(k) = f_{l_1 l_2}(k) + i I f_{l_1 l_2}(k), \quad (8)$$

which depend on the adiabatic parameter

$$k_{ii'22'} = \frac{2\pi c b}{v} (\omega_{ii'} + \omega_{22'}), \quad (9)$$

where $\omega_{ii'}$ and $\omega_{22'}$ are the transition frequencies in the absorbing and perturbing molecules, respectively. The same expression holds true for $S_{2f}^{\mathrm{outer}}(b)$ term. For the electrostatic potential (dipole-quadrupole and quadrupole-quadrupole interactions in our case) the functions $If(k)$ were calculated according to Ref. 28, for the induction and dispersion potential the imaginary part of resonance functions was calculated in Refs. 38. The expressions for $S_2^{\mathrm{middle}}(b)$ are similar.

Expression for $S(b)$ is invalid when b is small. We have used the cut procedure when b_0 is determined from the equation

$$\mathrm{Re}\, S(b_0) = 1. \quad (10)$$

$S(b) = 1$ for $b \le b_0$ and $S(b)$ is defined by formula (2) for $b > b_0$. Molecular parameters of H_2O, N_2, and O_2 molecules are presented in Table 1.

Table 1. Molecular parameters of H_2O, N_2, and O_2 molecules

Parameter	H_2O	N_2	O_2
μ, D	1.859	0	0
q, DÅ	2.9	3	0.7
Ω, DÅ^2	2	0	0
Φ, DÅ^3	0	6	8
α, 10^{-25} cm^3	14.69	17.6	16.1
ε, 10^{-11} erg	2.018	2.485	2.003
B_0, cm^{-1}	–	1.998	1.4456
D_0, cm^{-1}	–	$5.76 \cdot 10^{-6}$	$4.839 \cdot 10^{-6}$
$J_2^{\max}$	10	30	30

The H_2O molecular constants: dipole moments in the ground and in the first excited vibrational states were taken from Ref. 29, components of quadrupole moments – from Ref. 30, the dipole polarizability in the ground vibrational state – from Ref. 31.

The wave functions needed for determination of the matrix elements were calculated using the Watson rotational Hamiltonian, no Coriolis, Darling–Dennison or Fermi-type resonances were accounted for. The $i \to i'$, $f \to f'$ transitions, which are non-diagonal in vibrational quantum numbers, were neglected since they are much weaker than the pure rotational transitions. On the other hand, the corresponding transition frequencies $\omega_{ii'}$ and $\omega_{ff'}$ are large and this leads to small values of the

resonance functions and, as a consequence, to only small contribution to the shift value. To take into account centrifugal distortion corrections, we have used the effective dipole moment operator of the form[34]:

$$\mu = m_x^V \varphi_x + m_{x,x}^V \{\varphi_x, J_x^2\} + m_{x,y}^V \{\varphi_x, J_y^2\} + m_{x,z}^V \{\varphi_x, J_z^2\} + \\ + m_{y,xy}^V \{\varphi_y, \{J_x, J_y\}\} + m_{z,xz}^V \{\varphi_z, \{J_x, J_z\}\}, \quad (11)$$

where m are the numerical parameters dependent on vibrational state and J_x, J_y, J_z are the angular momentum operators. The mean dipole moment m_x^V for excited vibrational states was calculated according to formula

$$m_x^V = \langle V | \mu | V \rangle = \mu_e + \mu_1 v_1 + \mu_2 v_2 + \mu_3 v_3 \quad (12)$$

with the constants $\mu_e = -1.85498$; $\mu_1 = -0.00508$; $\mu_2 = -0.03166$; $\mu_3 = -0.02246$ D taken from Ref. 35. Other constants in Eq. (11) were assumed to be independent on vibrational state.[34] The quadrupole moment transition strengths for H_2O molecule have been calculated in the rigid rotor approximation.

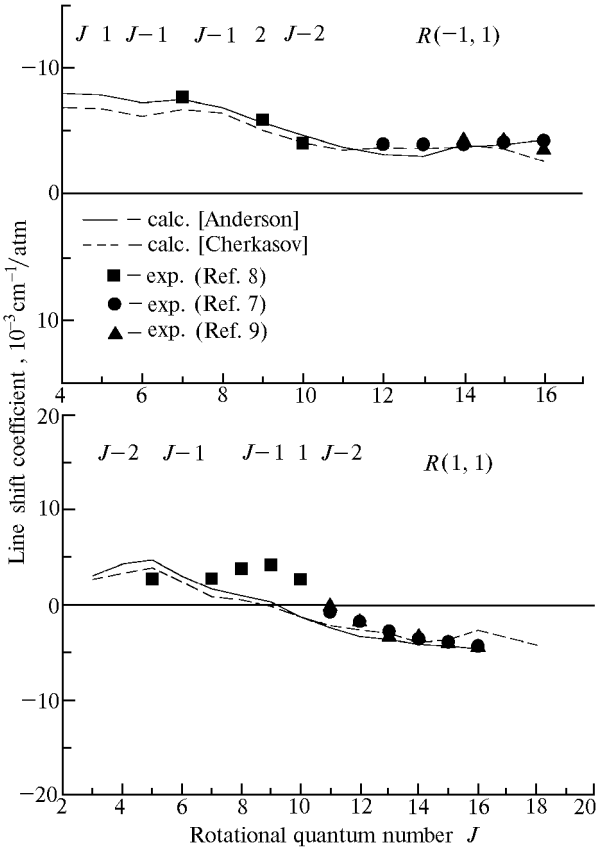

Fig. 1. Measured and calculated by two methods (Anderson and cut of free ones) line shift coefficients for $R(-1, 1)$ [J 1 $J-1 \leftarrow J-1$ 2 $J-2$] and $R(1, 1)$ [J 2 $J-1 \leftarrow J-1$ 1 $J-2$] sub-branches.

Since the comparison of line shift coefficients calculated by Anderson and Cherkasov (without cut procedure) methods shows their good agreement, we have used in the following analysis the Anderson method only. This method allows one to calculate separately different scattering channels and different interaction contributions. It is essential for the analysis of vibrational and rotational dependences of a line shift.

III. H_2O molecule line shifts

Vibrational dependence

As it has already been mentioned, the contributions of different terms of electrostatic potential for the $H_2O - H_2O$, $H_2O - N_2$, and $H_2O - O_2$ collisions were calculated separately. We have included into consideration the dipole-dipole, dipole-quadrupole, quadrupole-quadrupole, dipole-hexadecapole interactions, as well as the induction and dispersion terms of the polarization potential. For the case of the $H_2O - N_2$ and $H_2O - O_2$ collisions the calculations show that the main contribution to broadening and shifts of the pure rotational as well as belonging to fundamental bands transitions is due to interaction between the dipole moment of water and the quadrupole moment of nitrogen. The dipole–dipole interaction is the main term in the intramolecular potential which is responsible for the H_2O–H_2O broadening and shift in the low frequency region.

During the calculations the vibrational dependence of the molecular parameters such as the mean polarizabilities $\langle V_i | \alpha | V_i \rangle$ and $\langle V_f | \alpha | V_f \rangle$, the dipole moments $\langle V_i | \mu^2 | V_i \rangle$ and $\langle V_f | \mu^2 | V_f \rangle$, transition probabilities $D^2(ii' | l_1)$ and $D^2(ff' | l_1)$ as well as frequencies $\omega_{ii'}$ and $\omega_{ff'}$ have to be taken into account. For pure rotational transitions or for the transitions between the low lying vibration states the difference between mean polarizabilities of the upper and lower states is small, hence the $S_1(b)$ is small or even equal to zero. So the shift is determined mainly by the imaginary part of the $S_2(b)$. Vibrational excitation leads to the growth of the mean polarizability and, as a consequence, to an increase in the contribution to the shift value. The contribution from the $S_1(b)$ term then becomes strongly dependent on variation of the vibrational quantum numbers. The vibrational excitation changes also the second-order term $S_2(b)$ through the variation of the mean dipole moments as well as of the rotational and centrifugal distortion constants of the upper vibrational state. These effects become significant factors for line shifts of high overtones in the H_2O molecule, where the line shift is formed, in general, by the isotropic part of the intermolecular potential $S_1(b)$ ($S_1(b)$ is always negative) depending on the mean dipole polarizability in the upper vibrational state (see Fig. 2*b*). The same conclusion was drawn in Ref. 20, where the calculations were performed by Robert–Bonamy method that includes the short range forces into consideration.

Contributions to line shift coefficient from different parts of the intermolecular potential for two

bands: $3\nu_1 + \nu_3$ and ν_2 are presented in Fig. 2. It can be seen that in the $3\nu_1 + \nu_3$ band the J-dependence of a shift is mainly determined by the contribution coming from the polarization potential, in the ν_2 band – from the electrostatic potential, namely, from the dipole-quadrupole interaction.

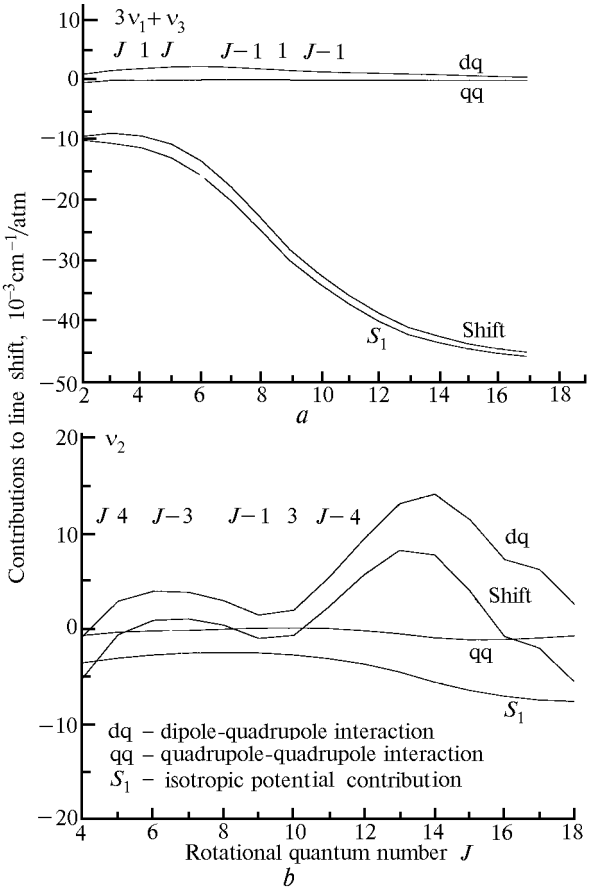

Fig. 2. Contributions to the line shift coefficient coming from different parts of the intermolecular potential for $3\nu_1 + \nu_3$ and ν_2 bands.

Rotational dependence of a shift and compensation for scattering channel contributions

Whereas the rotational dependence of the H_2O line broadening was a subject of a number of publications (see, for example, Ref. 9), there was no special study of rotational dependence of the water vapor line shift coefficient and its behavior at high values of rotational quantum numbers.

From the first sight, the behavior of measured line shift coefficients as a function of quantum number J looks chaotic: there is no definite J-dependencies. But if one selects the definite sub-branches according to definite combinations of the quantum numbers, such dependences are clearly seen. We selected different sub-branches in R–branch of ν_2 band: $R(1, 1)$, $R(1, -1)$, $R(-1, 1)$, $R(3, -1)$ (the first figure in parentheses equals to the change of K_a, the second – K_c). The set of sub-branches with different K_a quantum numbers is presented in Fig. 3. Such selection of the sub-branches allows us to explain the rotational dependence of a shift based on analysis of contributions from the scattering channel.

Molecular collisions result in mixing of different stationary state wave functions and thus one can say about collisionally induced transitions which reduce the level lifetime and lead to the additional line broadening and shift. The formulas of Anderson theory can be presented in the form which allows one to calculate separately contributions from different scattering channels. Traditionally one says about a scattering channel when two levels are connected by collisionally induced virtual transition. Henceforth we will use this terminology despite the fact that the transitions, which really take place, should interrupt the radiation process at a given frequency.

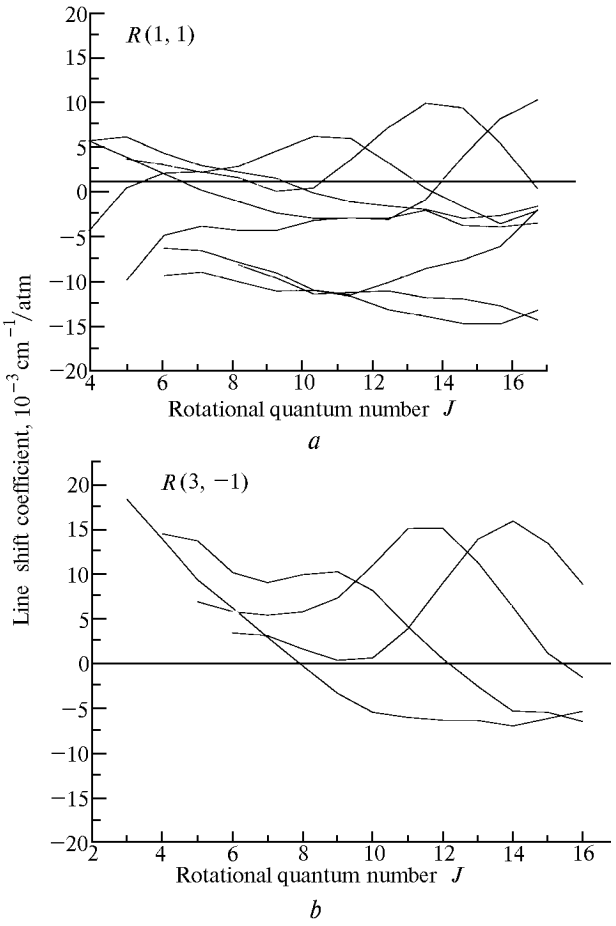

Fig. 3. Calculated line shift coefficients for $R(1, 1)$ and $R(3, -1)$ sub-branches.

It is obvious, that the contribution to the line width from each channel is positive.

As for the line shift, the contributions from different transitions may have opposite signs because the imaginary part of the resonance function is odd (depending on the sign of energy balance of the absorbing and perturbing molecules) and, as a concequence, partially cancel each other.

The contribution of a single scattering channel $i \to i'$ connected with the leading dipole-quadrupole interaction can be obtained from Eqs. (3)–(9)

$$\delta_{if} = \delta_i^{(1)} - \delta_f^{(1)} + \sum_{i'} D(ii' \mid 1)\, P_{\mathrm{dq}}(\omega_{ii'}) - \sum_{i'} D(ff' \mid 1) \times$$
$$\times\, P_{\mathrm{dq}}(\omega_{ff'}) = \delta_i^{(1)} - \delta_f^{(1)} + \sum_{i'} \delta_{\mathrm{dq}}^{ii'} - \sum_{f'} \delta_{\mathrm{qq}}^{ff'}, \quad (13)$$

and $P_{\mathrm{dq}}(\omega)$ depends on the parameters of perturbing particle and on the collision details (henceforth ω labels $\omega_{ii'}$ or $\omega_{ff'}$):

$$P_{\mathrm{dq}}(\omega) = -A_{\mathrm{dq}} \frac{n}{\hbar^2 c} \sum_2 \rho_2 \sum_{2'} D(22' \mid 2) \int_0^\infty v f(v)\, \mathrm{d}v \times$$
$$\times \int_{b_0}^\infty \frac{\mathrm{d}b}{v^2 b^5}\, I f_2 \left(\frac{2\pi c b}{v} (\omega + \omega_{22'}) \right). \quad (14)$$

The function $P_{\mathrm{dq}}(\omega)$ can be regarded as the effectiveness of the $i \to i'$ channel in shifts and it gives the Bweight@ of the transition considered in the line shift.

As was shown in Ref. 16, by direct calculations of $\delta_{\mathrm{dq}}^{ii'}$ and $\delta_{\mathrm{qq}}^{ff'}$, there is a compensation for the scattering channel contributions: the contribution of an individual channel to the line shift is often larger than the value of the line shift, but the contributions of different channels have different signs and they can partially cancel each other. The scheme of rotational levels for two different transitions in the $\nu_2 + \nu_3$ band is depicted in Fig. 4.

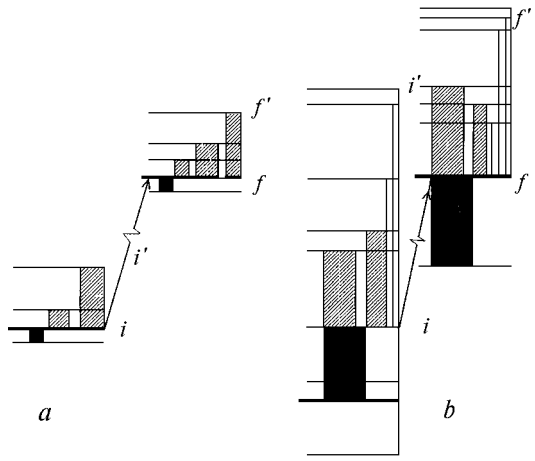

Fig. 4. The scheme of rotational levels of an absorbing molecule for two transitions with different values J in the band $\nu_1 + \nu_3$: $J = 4$ (*a*) and $J = 17$ (*b*).

The bar width is proportional to the scattering channel contribution value. It is seen that several leading contributions almost compensate each other so their total contribution to the shift becomes substantially smaller than some of the partial contributions. Besides, it can be seen that the compensation increases with the increasing rotational quantum number and, as a consequence, the electrostatic potential contributions are close to zero for the high J-values. Line shift coefficient is mainly determined by isotropic potential contribution.

According to Eqs. (13) and (14) the partial contribution is determined by direct product of $D^2(ii' \mid 1)/(2J_i + 1)$ and $P_{\mathrm{dq}}(\omega)$. Although the function $P_{\mathrm{dq}}(\omega)$ is a smooth function for the $H_2O - N_2$ system the J-dependence of the line shift coefficient is determined, first of all, by J-dependence of the dipole strengths.

Comparison of calculated shift values with the experimental data

Calculations of the line shift coefficients based on Anderson method were performed for water vapor lines broadened by N_2, O_2, and air in a wide spectral region from far IR to the visible range (Table 2). Line shift coefficients for the $\nu_2 + \nu_3$, $2\nu_2 + \nu_3$, $\nu_1 + \nu_3$, $2\nu_1$, $\nu_1 + \nu_2 + \nu_3$, $\nu_2 + 2\nu_3$ bands are presented in Table 3. The line shift coefficients in low frequency range are small (typically 10^{-3} cm^{-1}) and can be positive or negative, the situation is different in high frequency region where line shifts are always negative and have large values.

Table 2. The water vapor bands studied within Anderson theory

$v_1\ v_2\ v_3$	Band center, cm^{-1}	Number of lines	Pertuber	References
010	1594	70	N_2	9
110	5234	10	O_2	39
011	5331	28	O_2	«
		39	N_2	this paper
021	6871	20	N_2	«
200	7201	12	N_2	«
101	7249	25	N_2	«
012	9000	2	N_2	«
111	8807	36	N_2	«
301	13830	103	N_2	14
			O_2	«
			air	«
221	13652	42	N_2	«
			O_2	«
			air	«
202	13828	15	N_2	«
			O_2	«
			air	«
103	14318	3	N_2	«
			O_2	«
			air	«
401	17495	7	N_2	«
			O_2	«
			air	«

Table 3. The experimental and calculated line shift coefficients by nitrogen pressure ($10^{-3} \cdot cm^{-1}$/atm)

Line position, cm^{-1}	$v_1\ v_2\ v_3$	J''	K''_a	K''_c	J'	K'_a	K'_c	Experiment Ref. 10	2σ	Calculation
1	2	3	4	5	6	7	8	9	10	11
					2 μm					
5107.0703	011	9	3	7	10	3	8	−5.8	0.9	−10.0
5152.0993	011	7	1	6	8	1	7	−10.9	0.5	−10.6
5166.1931	011	7	5	3	8	5	4	−10.7	0.7	−11.0
5178.0992	011	6	4	2	7	4	3	−11.4	0.3	−8.6
5189.7198	011	5	3	2	6	3	3	−6.0	0.2	−5.3
5191.8791	011	6	5	1	7	5	2	−7.3	0.4	−11.8
5226.3515	011	4	1	4	5	1	5	−7.6	0.1	−8.0
5250.3091	011	4	0	4	4	2	3	−8.0	2.5	−11.3
5282.9623	011	6	2	5	6	2	4	−11.0	0.7	−4.8
5284.7803	011	1	0	1	2	0	2	−10.1	0.2	−7.9
5328.6310	011	6	3	4	6	3	3	−8.3	0.4	−5.5
5350.5344	011	6	4	3	6	4	2	−9.3	0.2	−10.7
5361.5245	011	7	5	3	7	5	2	−9.0	0.2	−12.6
5361.8928	011	7	5	2	7	5	3	−13.4	0.6	−11.1
5405.2906	011	5	1	4	5	1	5	−5.8	0.3	−7.9
5442.1522	011	4	3	1	3	3	0	−10.1	0.1	−10.5
5469.5269	011	6	2	5	5	2	4	−7.1	0.1	−6.7
5498.9953	011	6	4	2	5	4	1	−7.2	0.1	−9.4
5505.5546	011	8	2	7	7	2	6	−8.0	0.1	−8.0
5518.2874	011	7	3	4	1	3	3	−8.4	0.2	−6.0
5521.1385	011	7	4	4	6	4	3	−10.9	0.1	−10.2
5521.9039	011	9	2	8	8	2	7	−9.2	0.1	−8.7
5523.1329	011	9	1	8	8	1	7	−5.0	0.2	−7.2
5523.4538	011	7	4	3	6	4	2	−7.7	0.2	−6.9
5527.8448	011	8	3	6	7	3	5	−12.2	0.2	−9.6
5536.3074	011	8	2	6	7	2	5	−8.2	0.1	−5.5
5537.5414	011	10	2	9	9	2	8	−9.4	0.3	−9.7
5538.1290	011	10	1	9	9	1	8	−7.1	0.1	−8.4
5543.4219	011	8	4	5	7	4	4	−12.8	0.4	−10.0
5548.6557	011	8	4	4	7	4	3	−5.3	0.1	−5.7
5564.8228	011	9	4	6	8	4	5	−11.3	0.2	−10.5
5582.1670	011	11	3	9	10	3	8	−12.2	0.5	−11.9
5595.5578	011	10	3	7	9	3	6	−10.6	0.4	−7.8
					1.4 μm					
6705.0390	021	7	1	7	8	1	8	−10.7	0.7	−7.6
6726.2494	021	6	0	6	7	0	7	−12.2	0.1	−8.1
6727.2326	021	6	1	6	7	1	7	−12.2	0.5	−7.7
6748.8902	021	5	1	5	6	1	6	−8.3	0.3	−7.9
6753.5782	021	5	2	4	6	2	5	−3.7	0.5	−5.8
6799.3729	021	2	1	1	3	1	2	0.7	0.2	−1.7
6812.8111	021	2	1	2	3	1	3	−4.5	0.4	−5.8
6847.7267	021	0	0	0	1	0	1	−0.2	0.2	−0.6
6893.6485	021	2	2	0	2	2	1	−5.4	0.2	−1.0
6914.5496	021	4	3	2	4	3	1	−5.8	0.8	−5.7
6917.3693	021	2	0	2	1	0	1	1.5	0.2	1.7
6917.9525	021	2	1	2	1	1	1	−5.0	0.6	−3.5
6930.3670	021	2	1	1	1	1	0	−5.7	0.2	−6.5
6955.1576	021	4	0	4	3	0	3	0.2	0.1	−0.7
6956.3153	021	3	1	2	2	1	1	−5.3	0.4	−5.5
6963.1689	021	3	2	2	2	2	1	−3.8	0.3	−4.9
7004.2280	021	5	1	4	4	1	3	−0.6	0.6	−1.7
7006.1275	021	5	2	4	4	2	3	−6.9	0.2	−5.3
7025.3840	021	6	1	5	5	1	4	−2.5	0.3	−2.4
7034.4755	200	5	1	4	6	2	5	−10.1	0.4	−10.2
7063.1299	021	8	1	7	7	1	6	−5.8	0.9	−5.6
7070.7840	101	6	1	5	7	1	6	−11.6	0.1	−9.6
7079.1767	200	6	1	6	6	2	5	−5.8	0.9	−6.0
7080.5751	101	5	3	3	6	3	4	−4.4	0.1	−6.9
7104.6194	101	4	3	1	5	3	2	−3.8	0.2	−5.3
7108.7153	200	3	0	3	4	1	4	−10.9	0.2	−10.0
7120.3580	101	4	2	3	5	2	4	−8.0	0.2	−7.0
7127.0355	200	2	0	2	3	1	3	−8.0	0.4	−11.5

Table 3 (Continued)

1	2	3	4	5	6	7	8	9	10	11
7131.9505	200	3	1	3	3	2	2	−8.7	0.3	−9.6
7133.9031	101	3	3	0	4	3	1	−5.1	0.2	−4.1
7134.9821	101	3	3	1	4	3	2	−5.7	0.9	−4.6
7136.0941	101	3	2	1	4	2	2	−5.2	0.2	−5.3
7165.8211	101	2	2	0	3	2	1	−5.1	0.2	−6.3
7202.9098	101	1	0	1	2	0	2	−10.5	0.1	−9.0
7216.1909	101	5	4	1	5	4	2	−8.0	0.3	−8.6
7227.9685	101	4	3	2	4	3	1	−8.8	0.1	−7.8
7236.4474	200	2	2	0	2	1	1	−4.0	0.3	−2.0
7240.4159	101	2	2	1	2	2	0	−7.8	0.0	−7.6
7249.9247	200	2	2	1	2	1	2	−6.1	0.3	−7.5
7266.6518	200	3	3	1	3	2	2	−5.8	0.5	−0.0
7281.0820	200	4	1	4	3	0	3	−1.3	0.1	0.9
7283.7319	101	6	2	4	6	2	5	−5.0	0.2	−7.7
7286.0516	200	6	2	5	6	1	6	−4.3	0.9	−7.1
7305.0814	200	6	0	6	5	1	5	−8.0	0.4	−4.9
7312.1963	101	3	0	3	2	0	2	−3.9	2.0	−1.9
7323.9579	101	4	1	4	3	1	3	−6.9	0.1	−4.3
7331.7156	200	8	1	8	7	0	7	−10.0	0.4	−6.8
7348.4037	101	5	2	4	4	2	3	−12.3	0.3	−7.8
7351.4852	101	5	3	2	4	3	1	−5.8	0.2	−8.3
7359.3343	101	6	4	2	5	4	1	−6.7	0.2	−8.9
7378.6791	101	7	4	4	6	4	3	−10.2	0.2	−9.9
7397.5754	101	8	1	7	7	1	6	−6.5	0.1	−6.4
7403.6163	101	8	4	4	7	4	3	−4.1	0.3	−6.6
7406.0282	101	9	2	8	8	2	7	−13.8	0.2	−10.4
7407.7830	101	9	1	8	8	1	7	−8.4	0.4	−8.1
7413.0192	101	9	4	6	8	4	5	−12.8	0.6	−11.6
7417.8213	101	10	1	9	9	1	8	−7.6	0.3	−10.0
7419.1750	101	8	3	5	7	3	4	−11.4	0.3	−7.3
					1 μm					
8636.7581	111	6	1	5	7	1	6	−12.3	0.8	−11.6
8665.1311	111	5	2	4	6	2	5	−7.0	0.4	−9.8
8675.7803	111	5	1	5	6	1	6	−14.3	0.2	−11.3
8680.2591	111	4	1	3	5	1	4	−6.8	0.2	−8.7
8696.9877	111	4	0	4	5	0	5	−10.8	0.2	−10.9
8713.6592	111	3	2	2	4	2	3	−5.2	0.3	−6.7
8717.9110	111	3	0	3	4	0	4	−9.9	0.3	−10.3
8730.1318	111	2	1	1	3	1	2	−4.1	0.4	−4.3
8733.8083	111	2	2	0	3	2	1	−7.1	0.1	−6.6
8742.9292	111	2	1	2	3	1	3	−9.6	0.4	−8.8
8754.9302	111	1	0	1	2	1	1	−3.8	0.4	−4.8
8760.1410	111	1	0	1	2	0	2	−10.3	0.4	−10.0
8765.0406	111	1	1	1	2	1	1	−4.5	0.1	−7.5
8811.0630	111	2	2	0	2	2	1	−4.9	0.02	−6.4
8812.0143	111	4	3	1	4	3	2	−6.7	0.2	−8.6
8821.9196	111	5	5	0	5	5	1B	−14.2	0.6	−17.8
	111	5	5	1	5	5	0B			
8830.2319	111	1	0	1	0	0	0	−8.0	1.2	−8.0
8848.0705	111	2	1	2	1	1	1	−6.6	0.4	−6.2
8866.1671	111	3	1	3	2	1	2	−6.5	0.2	−5.2
8869.8731	111	3	0	3	2	0	2	−3.0	0.2	−3.0
8879.1198	111	3	2	2	2	2	1	−7.0	0.1	−8.5
8882.8726	111	4	1	4	3	1	3	−5.2	0.2	−5.5
8885.5740	111	4	0	4	3	0	3	−3.9	0.1	−3.5
8898.1943	111	5	1	5	4	1	4	−5.8	0.3	−6.1
8899.1304	111	4	2	3	3	2	2	−8.7	0.4	−8.9
8912.2568	111	6	1	6	5	1	5	−9.8	0.3	−7.3
8912.9834	111	6	0	6	5	0	5	−7.9	0.1	−6.3
8917.6803	111	5	2	4	4	2	3	−11.3	0.2	−9.0
8925.2222	111	7	1	7	6	1	6	−8.2	0.2	−8.9
8928.4787	111	5	3	3	4	3	2	−9.9	1.2	−12.3
8933.4633	111	5	2	3	4	2	2	−7.2	0.5	−8.6

Table 3 (Continued)

1	2	3	4	5	6	7	8	9	10	11
8934.7405	111	6	2	5	5	2	4	−12.0	0.6	−9.7
8948.4417	111	9	1	9	8	1	8	−12.4	0.5	−12.2
8950.3347	111	7	2	6	6	2	5	−13.3	0.3	−10.6
8956.2946	111	6	3	3	5	3	2	−7.5	0.4	−8.7
9350.3986	012	7	7	0	6	6	1B			
	012	7	7	1	6	6	0B	−27	3	−27

Note. B – blended lines.

Figure 5 presents J-dependence of the $R(1, 1)$ sub-branches for the $\nu_1 + \nu_2 + \nu_3$, $2\nu_1 + 2\nu_2 + \nu_3$, and $3\nu_1 + \nu_3$ bands. It can be seen from the figure that the rotational dependences of the similar transitions from different bands are alike but the lines with higher energy of the upper state have additional negative shift due to contribution of isotropic term of the intermolecular potential. Only one fitting parameter – the mean dipole polarizability in the upper state disturbed by incorrectness of the cut-procedure and short range effects of collisions was used in the calculations. For the H_2O–O_2 collision this parameter was taken from the H_2O–N_2 collision so this calculation can be regarded as predictable.

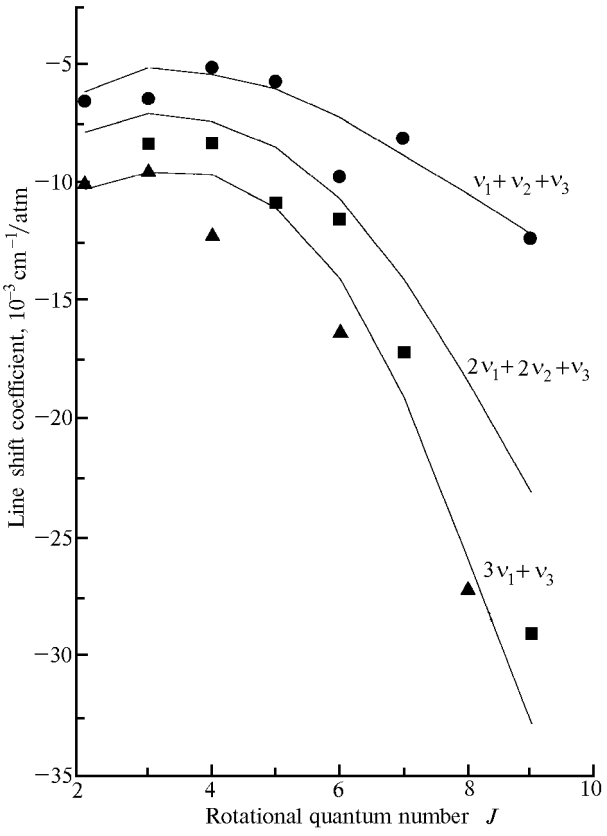

Fig. 5. The J-dependence of R (1, 1) sub–branches for the $\nu_1 + \nu_2 + \nu_3$, $2\nu_1 + 2\nu_2 + \nu_3$, and $3\nu_1 + \nu_3$ bands.

The agreement between calculations and experiment can be characterized by statistics of the observed and calculated values. The deviation from measured data for all water vapor lines presented in the Table 3 is given below:

$\Delta \le 0.0015$	73%
$0.0015 < \Delta \le 0.0030$	18
$0.0030 < \Delta \le 0.0045$	6
$0.0045 < \Delta \le 0.0060$	3

where $\Delta = |\delta^{obs} - \delta^{calc}|$.

IV. Conclusion

General conclusion which should be drawn from the experimental and calculated data available is that the water vapor line shifts can be characterized by strong vibrational and rotational dependences. Anderson theory allowed us to explain these peculiarities and to make calculations with good accuracy using only one fitting parameter. In spite of the simplicity of the Anderson method there is quite good agreement between the calculated and experimental line shift coefficients. The accuracy of the calculations is close to that of the calculations by Full Complex Implementation of Robert-Bonamy theory (FCRB), see Refs. 20–24.

Further development of the line shift coefficient calculations must be connected with correct analysis of the semiclassical impact theory (correctness of the cut procedure, short range potential contribution, trajectory bending) and some other effects, such as intermolecular interactions, which are important for water vapor molecule. Some analysis of these effects has been performed in Refs. 20–24, 36–38. To account for the trajectory curvature properly, the exact solutions of classical dynamic equations describing the relative motion of colliding molecules have been used to calculate the first- and second-order terms of the interruption function in Refs. 36–37. The calculations of resonance functions for the induction and dispersion potential needed for obtaining of higher order terms were calculated in Refs. 20 and 38.

Acknowledgments

The authors thank Corresponding Member of Russian Academy of Sciences S.D. Tvorogov for useful discussion of the problem of spectral line broadening and for financial support in the frame of Russian president grant “SchoolB No. 96–15–98. The work was

supported by the Russian Foundation of Basic Research (Grants No. 98–05–22021 and No. 98–02–16375).

References

1. E.W. Browell, in: *Optical and Laser Remote Sensing,* D.K. Jillinger and A. Mooradian, eds. (Springer–Verlag, Berlin, 1983), pp. 138–147.
2. V.V. Zuev, Yu.N. Ponomarev, A.M. Solodov, B.A. Tikhomirov, and O.A. Romanovsky, Opt. Lett. **10,** 318–320 (1985).
3. S.P. Belov, A.F. Krupnov, V.N. Markov, A.A. Mel'nikova, V.A. Skvortsov, M.Yu. Tret'yakov, J. Mol. Spectrosc. **101,** 258–270 (1983).
4. R.S. Eng, A.L. Calawa, T.C. Harman, P.L. Kelley, and A. Javan, Appl. Phys. Lett. **21**, 303–305 (1972).
5. R.S. Eng, P.L. Kelley, A. Mooradian, A.L. Calawa, and T.C. Harman, Chem. Phys. Lett. **19**, 524–528 (1973).
6. R.S. Eng, P.L. Kelley, A.Mooradian, and K.W. Nill, Mol. Phys. **28**, 653–664 (1974).
7. K.M.T. Yamada, M. Harter, and T. Giesen, J. Mol. Spectrosc. **157**, 84–94 (1993).
8. M.–A.H. Smith, Private communication.
9. A. Valentin, F. Rachet, A.D. Bykov, N.N. Lavrentieva, V.N. Saveliev, and L.N. Sinitsa, J. Quant. Spectrosc. Radiat. Transfer **59**, 165–170 (1998).
10. J.–P. Chevillard, J.–Y. Mandin, J.–M. Flaud, and C. Camy–Peyret, Can. J. Phys. **69**, 1286–1298 (1991).
11. V.G. Avetisov, A.I. Nadezhdinskii, A.N. Khusnutdinov, P.M. Omarova, and A.M. Zyrianov, J. Mol. Spectrosc. **160,** 326–334 (1993).
12. B.E. Grossman and E.V. Browell, J. Mol. Spectrosc. **136**, 264–294 (1989).
13. B.E. Grossman and E.V. Browell, J. Mol. Spectrosc. **138**, 562–595 (1989).
14. B.E. Grossman, E.V. Browell, A.D. Bykov, V.A. Kapitanov, V.V. Lazarev, Yu.N. Ponomarev, L.N. Sinitsa, E.A. Korotchenko, V.N. Stroinova, and B.A. Tikhomirov, Atm. Opt. **3**, 617–630 (1990).
15. R.R. Gamache, R. Lynch, J.J. Plateaux, and A. Barbe, J. Quant. Spectrosc. Radiat. Transfer **57**, 485–496 (1997).
16. A.D. Bykov, N.N. Lavrentieva, and L.N. Sinitsa, Opt. Spektrosk. **83**, 73–82 (1997).
17. A.D. Bykov, E.A. Korotchenko, Yu.S. Makushkin, Yu.N. Ponomarev, L.N. Sinitsa, A.M. Solodov, V.N. Stroinova, and B.A. Tikhomirov, Opt. Atm. **1**, No. 1, 40–46 (1988).
18. G. Buffa and O. Tarrini, J. Mol. Spectrosc. **101**, 271–277 (1983).
19. W.R. Davies, B.A. Oli, J. Quant. Spectrosc. Radiat. Transfer **20**, 95–120 (1978).
20. R. Lynch, R.R. Gamache, and S.P. Neshyba, J. Chem. Phys. **105**, 5711–5721 (1996).
21. R. Lynch, R.R. Gamache, and L.R. Brown, J. Quant. Spectrosc. Radiat. Transfer **56**, 471–487 (1996).
22. R. Lynch, R.R. Gamache, and S.P. Neshyba, J. Quant. Spectrosc. Radiat. Transfer **59**, 595–613 (1998).
23. R. Lynch, R.R. Gamache, and S.P. Neshyba, J. Quant. Spectrosc. Radiat. Transfer **59**, 615–626 (1998).
24. R. Lynch, R.R. Gamache, and S.P. Neshyba, J. Quant. Spectrosc. Radiat. Transfer **59**, 319–335 (1998).
25. P.W. Anderson, Phys. Rev. **76**, 657–661 (1949).
26. C.J. Tsao and B. Curnutte, J. Quant. Spectrosc. Radiat. Transfer **2**, 41–91 (1962).
27. M.R. Cherkasov, Opt. Spektrosk. **40**, 7–12 (1976).
28. D. Robert and J. Bonamy, J. de Phys. (Paris) **40**, 923–943 (1979).
29. C. Camy–Peyret and J.–M. Flaud, Mol. Phys. **32**, 523–537 (1971).
30. D.E. Stogryn and A.P. Stogryn, Mol. Phys. **11**, 371–393 (1966).
31. W.F. Murphy, J. Chem. Phys. **67**, 5877–5882 (1977).
32. C. Camy–Peyret and J.–M. Flaud, J. Mol. Spectrosc. **59**, 327–337 (1976).
33. J.–Y. Mandin, J.–P. Chevillard, and C. Camy–Peyret, J. Mol. Spectrosc. **116**, 168–190 (1986).
34. S.A. Clough, Y. Beers, G.P. Klein, and L.S. Rothman, J. Chem. Phys. **59**, 2254–2259 (1973).
35. S.L. Shostak and J.S. Muenter, J. Chem. Phys. **94**, 5883–5889 (1991).
36. A.D. Bykov, N.N. Lavrentieva, and L.N. Sinitsa, Atmos. Oceanic Opt. **4**, 587–594 (1992).
37. A.D. Bykov, N.N. Lavrentieva, and L.N. Sinitsa, Atmos. Oceanic Opt., **5**, 728–730 (1992).
38. A.D. Bykov and N.N. Lavrentieva, Atm. Opt. **4**, No. 7, 518–523 (1991).
39. N.N. Lavrentieva and A.M. Solodov, Proc. SPIE **3583**, 93–99 (1998).